Proc. Natl. Acad. Sci. USA
Vol. 90, pp. 567–571, January 1993
Medical Sciences

Alzheimer disease amyloid β protein forms calcium channels in bilayer membranes: Blockade by tromethamine and aluminum

(cation channel/phospholipid bilayer)

NELSON ARISPE, EDUARDO ROJAS, AND HARVEY B. POLLARD

Laboratory of Cell Biology and Genetics, National Institute of Diabetes and Digestive and Kidney Diseases, National Institutes of Health, Bethesda, MD 20892

Communicated by Bernhard Witkop, October 5, 1992 (received for review September 5, 1992)

ABSTRACT **Amyloid β protein (AβP) is the 40- to 42-residue polypeptide implicated in the pathogenesis of Alzheimer disease. We have incorporated this peptide into phosphatidylserine liposomes and then fused the liposomes with a planar bilayer. When incorporated into bilayers the AβP forms channels, which generate linear current–voltage relationships in symmetrical solutions. A permeability ratio, P_K/P_{Cl}, of 11 for the open AβP channel was estimated from the reversal potential of the channel current in asymmetrical KCl solutions. The permeability sequence for different cations, estimated from the reversal potential of the AβP-channel current for each system of asymmetrical solutions, is $P_{Cs} > P_{Li} > P_{Ca} \geq P_K > P_{Na}$. AβP-channel current (either Cs^+ or Ca^{2+} as charge carriers) is blocked reversibly by tromethamine (millimolar range) and irreversibly by Al^{3+} (micromolar range). The inhibition of the AβP-channel current by these two substances depends on transmembrane potential, suggesting that the mechanism of blockade involves direct interaction between tromethamine (or Al^{3+}) and sites within the AβP channel. Hitherto, AβP has been presumed to be neurotoxic. On the basis of the present data we suggest that the channel activity of the polypeptide may be responsible for some or all of its neurotoxic effects. We further propose that a useful strategy for drug discovery for treatment of Alzheimer disease may include screening compounds for their ability to block or otherwise modify AβP channels.**

Alzheimer disease (AD) is a chronic dementia affecting increasingly large numbers of the aging population. Pathologically, the brain is characterized by extracellular amyloid plaques, intraneuronal neurofibrillary tangles, and vascular and neuronal damage (1–7). The major component of brain amyloid plaques is a 39- to 42-residue peptide termed amyloid β protein (AβP) (8–12), which is a proteolytic product of amyloid precursor protein (APP). APP is a widely distributed membrane glycoprotein, defined by a locus on chromosome 21 (13, 14), in which mutations have been demonstrated in several cases of familial AD (7, 15). A C-terminal fragment of APP containing the AβP domain has been reported to be neurotoxic to neurons in culture (2, 16). Alternatively, it has been claimed that AβP is not itself toxic but that it potentiates neuronal sensitivity to neurotoxins (17–19). Finally, it has been claimed that toxicity may be mediated by interaction between AβP and neuronal serpin receptors, although such interactions do not appear to have intrinsic toxic consequences (7).

Previous reports have indicated that AβP disrupts calcium homeostasis and increases intraneuronal $[Ca^{2+}]_i$, and that the ability of the molecule to form neurofibrillar tangles could be the consequence of its ability to increase $[Ca^{2+}]_i$ (6). Furthermore, direct measurements of intracellular Ca^{2+} showed that cell exposure to AβP causes a rise in $[Ca^{2+}]_i$ (18). All of these observations, as well as the analysis of the primary and secondary structure of AβP (20), have led us to give consideration to the possibility that AβP might be an ion channel former.

METHODS

Bilayer Setup and Recording System. The experimental chamber (made of Plexiglas) consisted of two compartments separated by a thin Teflon film. Single channel currents were recorded using a patch clamp amplifier (Axopatch-1D, equipped with a CV-4B bilayer headstage; Axon Instruments, Burlingame, CA) and were stored on magnetic tape using a pulse code modulation/video cassette recorder digital system (Digital-4; Toshiba) with a frequency response in the range from dc to 25,000 Hz. Records were made from playbacks through a low-pass filter (eight-pole Bessel 902 LPF; Frequency Devices, Haverhill, MA) set in the range from 200 to 500 Hz.

Planar bilayers were formed by applying a suspension of synthetic palmitoyloleolylphosphatidylethanolamine and phosphatidylserine (50 mg/ml) in decane.

The AβP peptide, obtained from Bachem as β-amyloid [1-40] and dissolved in water at a concentration of 0.46 mM, was first incorporated into a suspension of pure phosphatidylserine liposomes by a method described elsewhere (21) and in the legend to Fig. 1. For channel studies, 5 μl of the liposome preparation containing the AβP peptide (*ca.* 5 μg of AβP) was added to the cis side of the chamber. To facilitate fusion of the liposomes with the bilayer, $CaCl_2$ (1 mM) was added to the solutions in both compartments. The concentration of free Ca^{2+} in the solutions was measured using a calcium electrode (CAL-1; W-P Instruments, New Haven, CT).

Data Analysis. Analysis of the records was carried out using a digital oscilloscope (Nicolet). In the majority of the incorporations ion channel activity occurred in more than one conductance state. To ascertain whether the duration of each event satisfied a criterion for the open state, we measured the amplitude of every discernable level at each transmembrane potential. The minimum acceptable time interval for defining an open-state level was taken as 20 ms.

The electrical potential of the solution in the cis compartment is referenced to that in the trans compartment, which was electrically connected to ground. Positive charge moving through the open channel from the trans to the cis side represents negative current. The data are a summary of 12–13 hr of recording.

RESULTS

The AβP Peptide Forms Cation-Selective Channels Across Bilayer Membranes. Discrete conductance changes, charac-

The publication costs of this article were defrayed in part by page charge payment. This article must therefore be hereby marked "*advertisement*" in accordance with 18 U.S.C. §1734 solely to indicate this fact.

Abbreviations: AβP, amyloid β protein; AD, Alzheimer disease; *I–V*, current–voltage.

teristic of ion channel activity, were always observed a few minutes after the addition of liposomes containing AβP to the cis compartment of the bilayer chamber. As illustrated in Fig. 1, in symmetrical CsCl solutions (in mM: 75 CsCl, 1 $CaCl_2$, 2 NaHepes, pH 7) changing the potential had no noticeable effects on the kinetics of the channel activity and on the number of levels at each transmembrane potential. Since complete AβP-channel closures from any one level occurred at −50, −30, and −20 mV, and frequent displacements of the current trace between different levels occurred at all potentials, we conclude that only one channel with multiple conductance levels was active in the bilayer.

To identify the charge on the ion carrying the current, we measured the shift in the reversal potential, V^*, induced by a change from a symmetrical to an asymmetrical KCl solution system. As shown in Fig. 2*A* (lower record) the kinetics of the AβP-channel activity was not affected by this change in [KCl]. However, at zero membrane potential a net negative current (positive charges moving from the trans to the cis side) of *ca.* −3 pA was measured (Fig. 2*A*, lower record). This result demonstrates that the ion carrying the bulk of the current is indeed K^+. The value of the new reversal potential, 8.5 mV (Fig. 2*B*), corresponds to a P_K/P_{Cl} of *ca.* 11.

Ca^{2+} Permeates the Open AβP Channel. To test whether Ca^{2+} permeates the open AβP channel we used the asymmetrical system of 37.5 mM CsCl in the cis compartment and 25 mM $CaCl_2$ in the trans compartment. At negative transmembrane potentials (−20 and −30 mV in Fig. 3*A*; −40 and

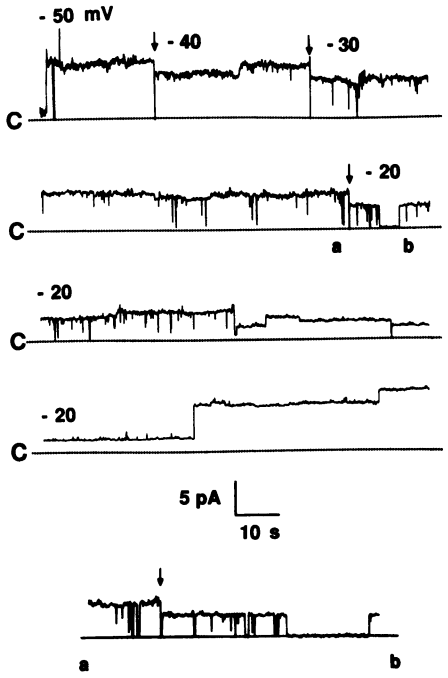

FIG. 1. Ion channel activity of AβP in a planar lipid bilayer. Transmembrane potential is given in mV above the corresponding current record. Symmetrical CsCl (75 mM, 1 mM $CaCl_2$, 2 CsHepes, pH 7) solutions were used. Vertical arrows indicate 10-mV step changes in membrane potential. To determine the conductance of the AβP channel, a linear current–voltage (*I–V*) curve with a slope of 206 pS was drawn by eye to intercept the potential axis at 0 mV (not shown). At the bottom, the segment a–b, from the second record, is shown on an expanded time base, where the time calibration representing 10 s on the upper records now represents 2.2 s. To prepare liposomes 20 μl of phosphatidylserine (Avanti Polar Lipids) dissolved in chloroform (10 mg/ml) was placed in a tube. After evaporation of the chloroform by blowing nitrogen gas, 30 μl of 1 M potassium aspartate (pH adjusted to 7.2) was added and the resulting mixture was sonicated for 5 min. Next, 20 μl of the AβP stock solution (2 mg/ml) in water was added and the adduct was sonicated for 2 further min.

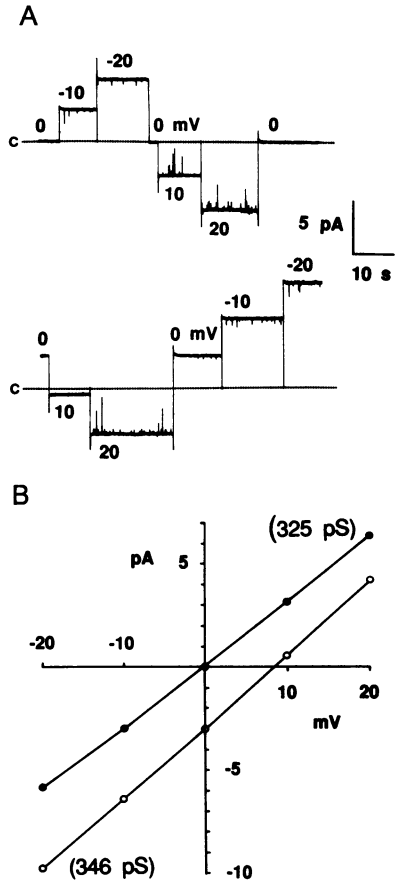

FIG. 2. The AβP channel is cation-specific. (*A*) The upper record of the AβP-channel activity was made in a symmetric system of 40 mM KCl (1 mM $CaCl_2$, 2 mM NaHepes, pH 7). The transmembrane potential (in mV) is indicated next to the corresponding current record. The lower record was made after the increase $[KCl]_{trans}$ from 40 to 60 mM. (*B*) Amplitude of the AβP-channel current (in pA) is plotted as a function of transmembrane potential (in mV). Each point of the *I–V* curve represents the mean value of at least three readings of the amplitude of the current at the potential indicated. Channel conductance was *ca.* 325 pS (●) in symmetrical (40 mM KCl) and 346 pS (○) in asymmetrical (40 and 60 mM KCl) solutions, respectively. Intercepts are at 0 (●) and 8.5 mV (○), respectively. The intercept, V^*, may be used to estimate P_K/P_{Cl} using the following equation: $V^* = RT/F\ln\{P_K[K]_t + P_{Cl}[Cl]_c\}/\{P_K[K]_c + P_{Cl}[Cl]_t\}$, where $[X]_t$ and $[X]_c$ are the concentrations of the ion species X in the trans and cis compartments, respectively; *F*, *R*, and *T* have their usual meanings (22). Inserting the values for the concentrations ($[K]_t$ = 60 mM, $[K]_c$ = 40 mM, $[Cl]_t$ = 60 mM, and $[Cl]_c$ = 40 mM) into the equation, we get P_K/P_{Cl} = 11.

−60 mV in Fig. 3*B*) distinct, discrete jumps in the current record between different levels were observed. At potentials negative to −4 mV, currents representing Ca^{2+} flowing from the trans to the cis side through the open AβP channel were recorded.

Fig. 3*B* illustrates another interesting property of the AβP channel. Repetitive applications of step changes in potential from 0 to either −40 mV (Fig. 3*B*, upper records 1–3) or −60 mV (lower records 1, 2 A and B, 3) always induced the appearance of different Ca^{2+} current levels. In all cases, the size of the initial current jump was higher than that eventually attained. However, the duration of the initial current jump was shortened with increasing magnitude of the potential (Fig. 3*B*). This behavior was only seen if Ca^{2+} was the charge carrier. Finally, we noted that complete AβP-channel closures could be observed to occur from any one level to the closed states. These changes are shown for the −60 mV records in Fig. 3*B* (records 2 A and B). These frequent

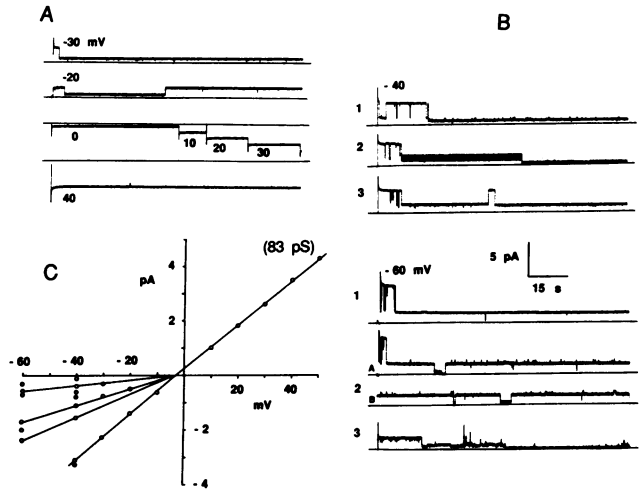

FIG. 3. The AβP channel is permeable to Ca^{2+}. (*A*) Segments of a continuous record of the AβP-channel activity at different potentials. Solution in the cis compartment contained (in mM) 37.5 CsCl, 1 $CaCl_2$, 1 CsHepes, pH 7; the trans compartment contained (in mM) 25 $CaCl_2$, 2 NaHepes, pH 7. (*B*) Records labeled 1–3 (*B*, upper and lower panels) are continued from those in *A*. Ca^{2+} is the charge carrier at negative potentials and Cs^+ at positive potentials. The numbers on the left side of each record indicate the order in which the same step was applied (either from 0 to −40 or to −60 mV). (*C*) The amplitude of the current (in pA) is plotted as a function of the transmembrane potential (in mV). Each point on the *I–V* curve represents either the mean value of two or three readings of the amplitude of the AβP-channel current at positive potentials (Cs^+ current) or single readings at negative potentials (Ca^{2+} current). The permeability ratio P_{Ca}/P_{Cs} is computed to be 0.6 from the equation (22): $V^* = RT/F\ln\{4P'_{Ca}[Ca]_t\}/\{P_{Cs}[Cs]_c + 4P'_{Ca}[Ca]_c\exp^{V^*F/RT}\}$, where $P'_{Ca} = P_{Ca}/\{1 + e^{V^*F/RT}\}$ and where $V^* = -4$ mV, $[Ca]_t = 25$ mM, $[Ca]_c = 1$ mM, $[Cs]_c = 37.5$ mM.

displacements of the Ca^{2+} current trace between different levels suggest that only one channel with multiple conductance levels is active in the bilayer. At positive membrane potentials, with Cs^+ carrying the current, the conductance of the AβP channel was estimated to be 83 pS (Fig. 3*C*, o). By contrast, in symmetrical 75 mM CsCl solutions (Fig. 1), the conductance was estimated as *ca.* 206 pS.

Permeability Sequence for Cations. To determine the sequence of permeabilities for different cations, including Cs^+, Na^+, K^+, Li^+, and Ca^{2+}, we recorded AβP-channel currents at different transmembrane potentials under conditions of solution asymmetry. We then measured the amplitude of channel events at each membrane potential and constructed *I–V* curves. P_{Ca}/P_{Cs} can be computed from the data in Fig. 3*C* to be 0.6, using the equation given in the legend to Fig. 3*C*.

As expected for a cation-selective channel, the conductance of the AβP channel in the asymmetrical system depends on the cation carrying the current. Fig. 4*A* shows AβP-channel current records made with 37.5 mM LiCl in the trans compartment and 37.5 mM CsCl in the cis compartment. At zero potential across the bilayer a net positive current is observed (Fig. 4*A*). Furthermore, with Cs^+ as charge carrier the conductance is *ca.* 264 pS (Fig. 4*B*, straight line through the points at 0, 10, and 20 mV) and *ca.* 181 pS with Li^+ as charge carrier (Fig. 4*B*, points at −40, −30, −20, and −14 mV). Thus, the conductance of the AβP channel with Cs^+ as charge carrier is *ca.* 1.5 times greater than that with Li^+ as the charge carrier. From the value of the reversal potential of −14 mV in Fig. 4*B*, we calculate a P_{Cs}/P_{Li} of *ca.* 1.6.

We also noted the preferential flow of Ca^{2+} and K^+ over Na^+ through the open AβP channel (see Fig. 5). A detailed study showed that P_K/P_{Na} and P_{Ca}/P_{Na} were 1.3.

In symmetrical 75 mM CsCl (Fig. 1) and asymmetrical 37.5 mM CsCl/LiCl (Fig. 4) solutions, the average conductance of the AβP channel (with Cs^+ as the charge carrier) was found to be *ca.* 235 pS. In contrast, in the asymmetric system 37.5 mM CsCl/25 mM $CaCl_2$ (Fig. 3), with Cs^+ as the charge carrier, the conductance was only 83 pS. This apparent blockade by Ca^{2+} of the flow of Cs^+ through the AβP channel was further studied directly in the experiment illustrated in Fig. 6. Control records of the channel activity were made at ±60, ±40, and ±20 mV (Fig. 6*A*). Next, the concentration of Ca^{2+} in the cis compartment was augmented from 1 to 10 mM and a second family of records was made. As shown in Fig. 6*B*, the amplitude of the channel current and the frequency of openings were drastically reduced by Ca^{2+}. Fig. 6*B* also shows that the current flowing through the open, but blocked, AβP channel is rectified—i.e., at −60 mV the magnitude of Cs^+ current is larger than at 60 mV.

The permeability ratios obtained so far can be used to establish a permeability sequence for the different cations tested. We know that $P_K/P_{Na} = P_{Ca}/P_{Na} = 1.3$ (Fig. 5). It follows that $P_{Ca} = P_K = 1.3\ P_{Na}$. Furthermore, we also know that $P_{Ca}/P_{Cs} = 0.6$ (or, $P_{Cs}/P_{Ca} = 1.67$) and $P_{Cs}/P_{Li} = 1.6$ (Figs. 3 and 4). The product of these two ratios eliminates P_{Cs} and gives $P_{Ca}/P_{Li} = 0.96$. Eliminating P_{Ca} from the ratios $P_{Ca}/P_{Cs} = 0.6$ (Fig. 3) and $P_{Ca}/P_{Na} = 1.3$ (Fig. 3), we obtain $P_{Na}/P_{Cs} = 0.46$. Thus, the complete permeability sequence is $P_{Cs} > P_{Li} > P_{Ca} = P_K > P_{Na}$.

Blockade of the AβP-Channel Activity by Tromethamine and Al^{3+}. As part of our studies of the cationic permeability sequence through the AβP channel, we noted that tromethamine not only was impermeable but also actually blocked the channel currents. Fig. 7*A* illustrates the blockade by tromethamine (10 mM) of the channel currents with either Ca^{2+} (records at −20, −10, and 0 mV) or Cs^+ (records at 10

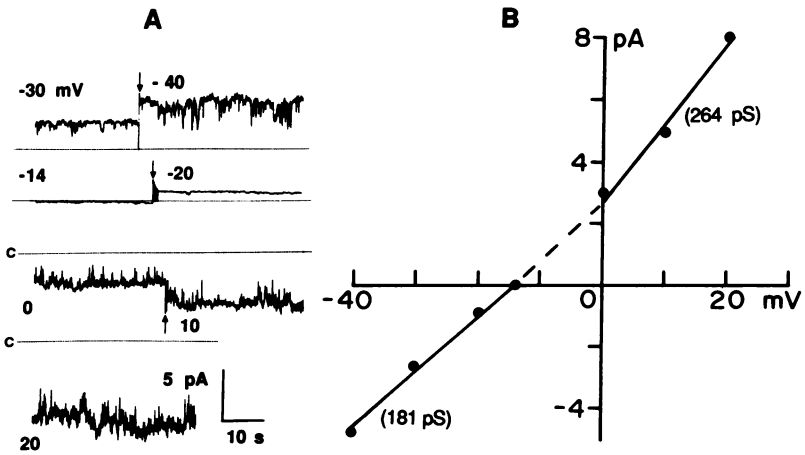

FIG. 4. Li^+ is permeable through the AβP channel. (*A*) Sample records of the AβP-channel activity at different potentials. Vertical arrows indicate a step change in membrane potential. (*B*) Each point (●) of the *I–V* curve represents the mean value of two or three readings of the amplitude of the current at the potential indicated. Composition of the solution in the cis compartment is (in mM) 37.5 CsCl, 1 $CaCl_2$, 2 NaHepes, pH 7; composition in the trans compartment is (in mM) 37.5 LiCl, 1 $CaCl_2$, 2 NaHepes, pH 7. The numbers in parentheses next to the lines represent the channel conductance.

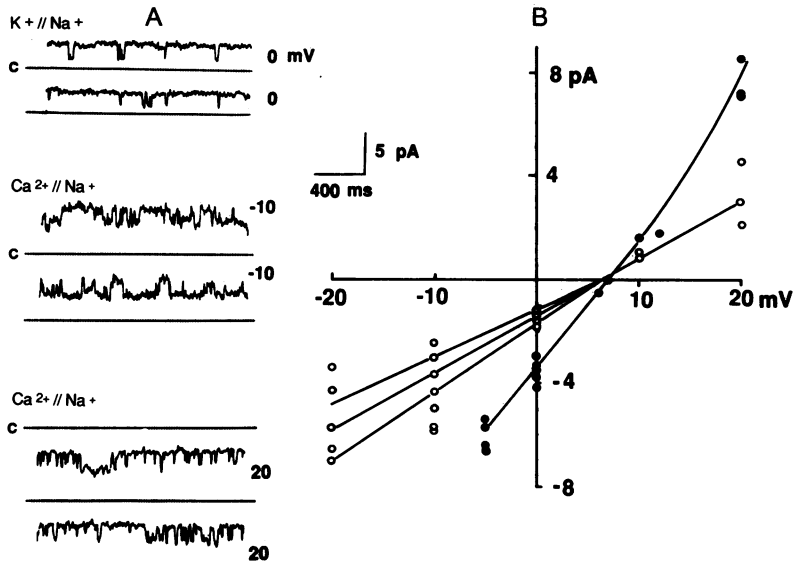

FIG. 5. Preferential flow of K^+ and Ca^{2+} over Na^+ across the open AβP channel. Initially channel activity was recorded with the asymmetrical system of a KCl solution in the trans compartment (in mM: 40 KCl, 1 $CaCl_2$, 2 NaHepes, pH 7) and a NaCl solution in the cis side (in mM: 40 NaCl, 1 $CaCl_2$, 2 NaHepes, pH 7). Keeping the composition of the solution in the cis side constant, the solution in the trans compartment was replaced by a $CaCl_2$ solution (in mM: 25 $CaCl_2$, 2 NaHepes, pH 7). A few minutes later channel activity was recorded at different potentials. (*A*) Sample records of the AβP-channel activity with either K^+ (top pair), Ca^{2+} (middle pair), or Na^+ (lower pair) as charge carrier. (*B*) The amplitude of the current (in pA) is plotted as a function of membrane potential (in mV). Each point on the *I–V* curve represents the mean value of two or three readings of the amplitude of the AβP-channel current for the KCl/NaCl system (●) and for the $CaCl_2$/NaCl system (○). Note that the lines joining the experimental points intercept the horizontal axis at *ca.* 7 mV.

and 20 mV) carrying the current. Addition of tromethamine (10 mM) to the cis side drastically reduced the amplitude of the currents as well as the frequency of the channel events (see Fig. 7*A*, 6th to 10th records from the top) at ±20 and −40 mV.

Since AβP in amyloid plaques is known to bind Al^{3+}, we also tested the AβP channels for sensitivity to aluminum. As shown in Fig. 7 *B* and *C*, addition of Al^{3+} (10 or 20 μM) blocked the channel activity. Blockade of the AβP channel by a high dose of Al^{3+} (1 mM; Fig. 1*D*) was rapid, and the blockade persisted at high potentials (±60 mV).

DISCUSSION

The present results demonstrate that synthetic AβP forms cation-selective channels across planar lipid bilayers. The permeability sequence (P_{Ca} as reference) is $P_{Ca} = 0.6 \times P_{Cs} = 0.96 \times P_{Li} = P_K = 1.3 \times P_{Na}$. Taking P_{Na} as reference, the sequence is $P_{Na} = 0.46 \times P_{Cs} = 0.74 \times P_{Li} = 0.77 \times P_K$. The AβP channel is therefore permeable to all monovalent metal ions tested. This property is not uncommon in other classical Ca^{2+} channels, including the voltage-gated L-type Ca^{2+} channel present in the plasma membrane (23) and the Ca^{2+} release channel of the endoplasmic reticulum (24). However, permeation by these monovalent cations through conventional Ca^{2+} channels, when studied in Ca^{2+}-free solutions, ceases if calcium in the micromolar range is added (23). In contrast, we found that in the presence of Ca^{2+} (1 mM) the AβP channel is permeable to K^+, Cs^+, Na^+, and Li^+. However, we did find that increasing [Ca^{2+}] from 1 to 10 mM in one compartment leads to voltage-dependent blockade of channel activity (Fig. 6*B*). Therefore, at least on a qualitative basis, both types of Ca^{2+} channels share a common mode of interaction with monovalent cations and calcium. Based on the available data, it may be most appropriate to use the multi-ion channel model to explain the behavior of the AβP channel (23). This model may also explain the slightly asymmetric blockade of AβP channels by either tromethamine or aluminum (Fig. 7).

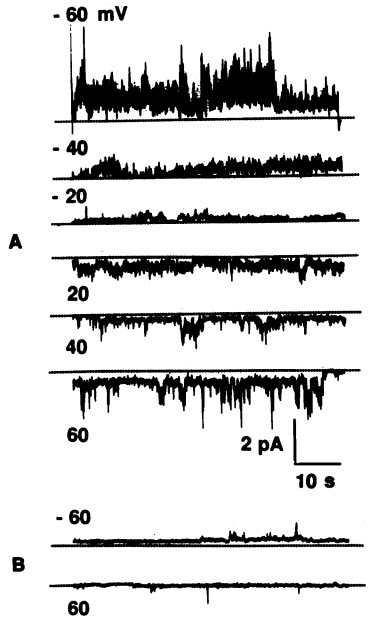

FIG. 6. Effects of Ca^{2+} on AβP-channel activity. (*A*) The AβP-channel activity was recorded using the symmetrical system of 200 mM CsCl (in mM: 200 CsCl, 1 $CaCl_2$, 2 NaHepes, pH 7). Control current records were gathered at ±60, ±40, and ±20 mV. (*B*) The concentration of Ca^{2+} in the cis compartment was then increased from 1 to 10 mM, and another series of records were made 10 min later. Representative records at ±60 mV are shown.

We have also given some consideration to the question of how a peptide of only 40 amino acids might form a calcium channel with such characteristic properties. It is possible that more than one AβP molecule may form a channel, since in water synthetic AβP forms stable dimers (25) or dimers, trimers, and tetramers (20). Thus, any of these forms could constitute the channel, and these different possibilities could lead to the variable kinetic and conductive properties of the AβP channel. Barrow *et al.* (20) emphasize that synthetic AβP can express different proportions of α-helix and β-sheet, depending on physiologically relevant environmental variables such as ionic strength, pH, and hydrophobicity. Finally, Kang *et al.* (26) have also suggested, on the basis of molecular considerations, that AβP could span the membrane through a C-terminal hydrophobic α-helical domain, leaving free the N-terminal β-sheet domain.

The finding that AβP has intrinsic Ca^{2+}-channel activity leads to the obvious question of whether the channel could be the basis of any AβP-derived neuronal or endothelial injury in AD. Indeed, a disordered Ca^{2+} homeostasis, either directly or indirectly, has been viewed as a toxic effect of AβP leading to AD (6, 18).

Finally, if the ion channel activity of AβP indeed has anything to do with the pathogenesis of AD, tromethamine, or a similarly efficacious compound, could be considered a candidate therapeutic agent. Tromethamine is a relatively nontoxic substance (LD_{50} in mice = *ca.* 0.5 g/kg), having a history of therapeutic use at high concentrations in humans

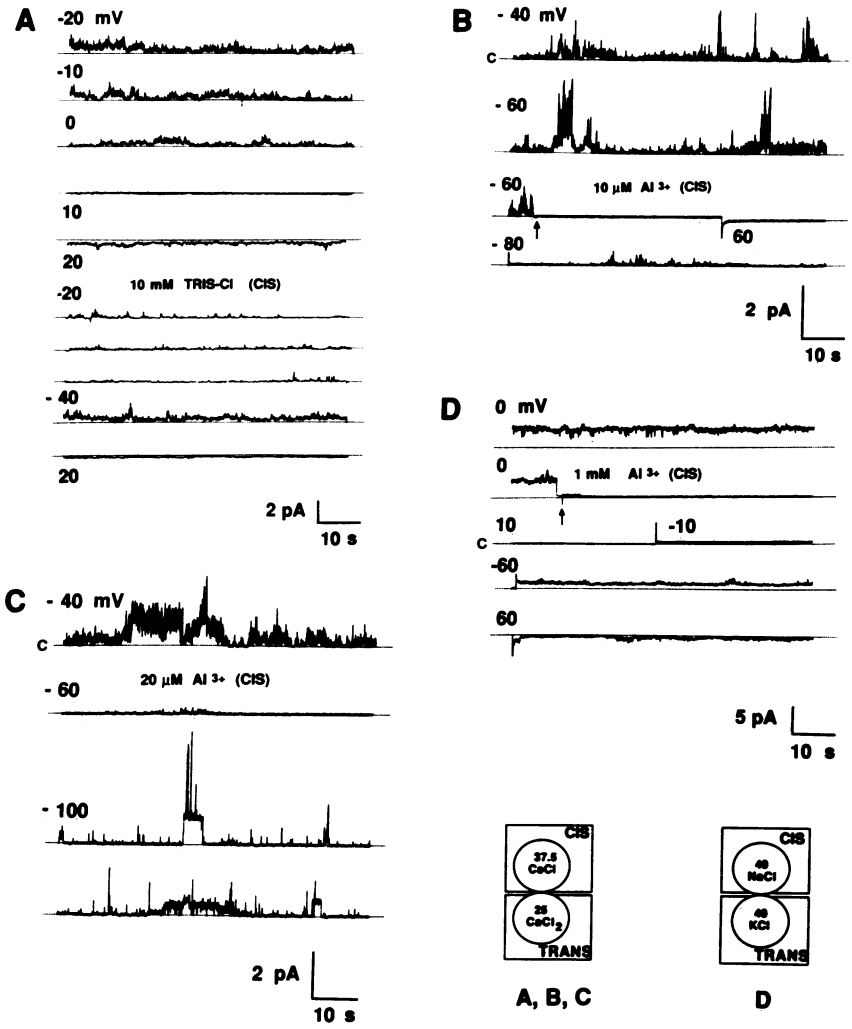

FIG. 7. Tromethamine and aluminum block AβP channels. For *A–C* the asymmetrical 37.5 mM CsCl/25 mM $CaCl_2$ system was used (2 mM Na-Hepes, pH 7, both compartments; 1 mM $CaCl_2$ cis side). For *D*, the asymmetrical 40 mM NaCl/40 mM KCl system was used (1 mM $CaCl_2$, 2 mM NaHepes, pH 7, both compartments). (*A*) Control channel activity at ±20, ±10, and 0 mV prior to the addition of tromethamine (upper records). Tromethamine (10 mM, as Tris·HCl, pH 7) was added to the cis side, and remaining channel activity was recorded after 1–2 min at ±20 and −40 mV. (*B*) Sample records of control channel activity gathered at −40 and −60 mV (upper two records) under the same conditions as for *A*. $Al_2(SO_4)_3$ (10 μM) was added to the cis compartment, and channel activity was recorded *ca.* 3 min later. The lower two records are representative of the remaining channel activity at −60 and −80 mV. (*C*) Control channel activity is shown at −40 mV, under the same conditions as *A* and *B*. $Al_2(SO_4)_3$ (20 μM) was added to the cis side, and records were made *ca.* 3–5 min later. No channel activity could be detected at −40 mV, and the records shown at −60 and −100 mV illustrate the potency of aluminum as a blocker of the AβP channel. (*D*) Control channel activity is shown at 0 mV, in the asymmetrical 40 NaCl/KCl system. Upon addition of $Al_2(SO_4)_3$ (1 mM) to the cis compartment, channel activity was substantially attenuated.

for metabolic and respiratory acidosis (27) and use in electrophysiological studies of Na^+-channel gating as an impermeant, nontoxic substitute for Na^+ (28). In this manner, the AD AβP calcium channel system could serve as a convenient and possibly relevant platform for further efforts at drug discovery and development.

1. Blessed, G., Tomlinson, B. E. & Roth, M. (1968) *Br. J. Psych.* **114,** 797–811.
2. Neve, R. L., Dawes, L. R., Yankner, B. A., Benowitz, L. I., Rodriguez, W. & Higgins, G. A. (1990) *Prog. Brain Res.* **86,** 257–267.
3. Katzman, R. & Saitoh, T. (1991) *FASEB J.* **5,** 278–286.
4. Selkoe, D. J. (1991) *Neuron* **8,** 487–496.
5. McKee, A. C., Kosik, K. S. & Kowall, N. W. (1991) *Ann. Neurol.* **30,** 156–165.
6. Hardy, J. A. & Higgins, G. A. (1992) *Science* **256,** 184–185.
7. Kosik, K. S. (1992) *Science* **256,** 780–783.
8. Roth, M., Tomlinson, B. E. & Blessed, G. (1966) *Nature (London)* **209,** 109–110.
9. Terry, R. D., Peck, A., DeTeresa, R., Schechter, R. & Horoupian, D. S. (1981) *Ann. Neurol.* **10,** 184–192.
10. Glenner, G. G. & Wong, C. W. (1964) *Biochem. Biophys. Res. Commun.* **120,** 885–890.
11. Masters, C. L., Simms, G., Weinman, N. A., Multhaup, G., McDonald, B. L. & Beyreuther, K. (1985) *Proc. Natl. Acad. Sci. USA* **82,** 4245–4249.
12. Joachim, C. L., Duffy, L. K. & Selkoe, D. (1988) *Brain Res.* **474,** 100–111.
13. Goldgaber, D., Lerman, M. I., McBride, O. W., Saffiotti, U. & Gajdusek, C. (1987) *Science* **235,** 877–880.
14. Tanzi, R. E., Gusella, J. F., Watkins, P. C., Bruns, G. A. P., St. George-Hyslop, P., Van Keuren, M. L., Patterson, D., Pagan, S., Kurnit, D. M. & Neve, R. L. (1987) *Science* **235,** 880–882.
15. Goate, A., Chadier-Harlin, M.-C., Mullan, M., Brown, J., Crawford, F., Fidani, L., Giuffra, L., Haynes, A., Irving, N., James, L., Mant, R., Newton, P., Rooke, K., Roques, P., Talbot, C., Rossor, M., Owen, M. & Hardy, J. (1991) *Nature (London)* **349,** 704–706.
16. Yankner, B. L., Duffy, L. K. & Kirschner, D. A. (1990) *Science* **250,** 279–282.
17. Koh, J. Y., Yang, L. L. & Cotman, C. W. (1990) *Brain Res.* **533,** 315–320.
18. Mattson, M. P., Cheng, B., Davis, D., Bryant, K., Lieberburg, I. & Rydel, R. E. (1992) *J. Neurosci.* **12,** 376–389.
19. Pike, C. J., Walencewitz, A. J., Glabe, C. G. & Cotman, C. W. (1991) *Brain Res.* **563,** 311–314.
20. Barrow, C. J., Yasuda, A., Kenny, T. M. & Zagorski, M. G. (1992) *J. Mol. Biol.* **225,** 1075–1093.
21. Arispe, N., Rojas, E. & Pollard, H. B. (1992) *Proc. Natl. Acad. Sci. USA* **89,** 1539–1543.
22. Lakshminarayanaiah, N. (1984) *Equations of Membrane Biophysics* (Academic, Orlando, FL).
23. Tsien, R. W., Hess, P., McCleskey, E. W. & Rosenberg, R. L. (1987) *Annu. Rev. Biophys. Biophys. Chem.* **16,** 265–290.
24. Suarez-Isla, B. A., Alcayaga, C., Marengo, J. J. & Bull, R. (1991) *J. Physiol. (London)* **441,** 575–591.
25. Hilbich, C., Kisters-Woike, B., Reed, J., Masters, C. L. & Beyreuther, K. (1991) *J. Mol. Biol.* **218,** 149–163.
26. Kang, J., Lemaire, H.-G., Unterbeck, A., Salbaum, J. M., Masters, C. L., Grzeschik, K.-H., Mulhaup, G., Beyreuther, K. & Muller-Hill, B. (1987) *Nature (London)* **325,** 733–736.
27. Nahas, G. G. (1962) *Pharmacol. Rev.* **14,** 447–472.
28. Keynes, R. D., Rojas, E. & Cena, V. (1991) *Proc. R. Soc. London B* **246,** 129–133.